

Physical effect of annealing conditions on soluble organic semiconductor for organic thin film transistors

**Dongwoo Kim, Doohyun Kim, Keonsoo Kim, Hyungjin Kim, Donghyuck Lee
and MunPyo Hong***

Dept. of Display and Semiconductor Physics, Korea University, Chungnam, KOREA

TEL: 82-41-860-1321, e-mail: goodmoon@korea.ac.kr

Keywords: OTFT, Drying Process, Annealing Condition, Soluble Organic Semiconductor

Abstract

We have examined the effect of physical drying and annealing conditions for the soluble derivatives of polythiophene as p-type channel materials of organic thin film transistors (OTFTs) in our special designed drying system; performances of the jetting-processed OTFTs can be improved more than 10 times just by optimizing the physical conditions of drying and annealing.

1. Introduction

Recently, Organic thin-film transistors (OTFTs) have been researched for many applications such as sensors, smart cards, identification tags, and the display devices including flexible displays.[1] Also, Ink-jet printing has received special attention as a direct patterning technique for the cost-effective fabrication of organic electronic devices such as organic light-emitting diodes (OLEDs), organic field effect transistors (OFETs), and organic photovoltaic (OPVs). Previous studies on ink-jet-printed electronics have mainly focused on the printing of conducting materials, such as conducting polymers and inks based on metal nanoparticles as electrodes in circuits,[2]. However, a significant step toward achieving ink-jet-printed electronics would be the development of a printing method for semiconducting materials. In this paper, we have investigated the soluble process through a drying system for the soluble OSC film as a practical semiconductor for mass-productions and compared with well-known OSC materials such as 6,13-bis((triisopropylsilyl)ethynyl) pentacene,[3] and Poly(3-hexylthiophene), which have higher high occupy molecular orbital (HOMO) as above 5.0 eV. For enhancement of crystallite properties of soluble OSC, its crystallites are improved by optimized jetting process with post solvent annealing.

2. Experimental Procedure

To compare effects of the drying mechanism in the soluble OSC material itself, we fabricated bottom contact OTFT devices with circle type source-drain electrode by solution jetting process as shown in Fig.1.

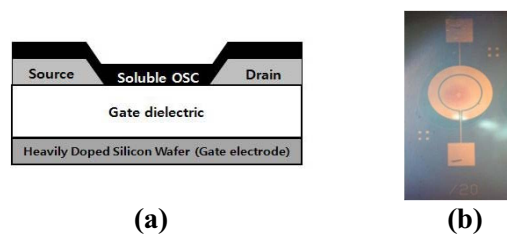


Figure 1. Configurations of (a) bottom-gate & bottom contact structure and (b) circle type source-drain electrode

The thermally oxidized silicon dioxide (SiO_2) wafer with the total thickness about 3000 Å was prepared. The OTFTs devices are fabricated for a bottom contact configuration on a degenerately doped n^+ silicon wafer used as a gate electrode. For the formation of circle type source-drain electrodes, Au metal layer was deposited by a thermal evaporation with thickness of 300 Å, and patterned by photolithography and wet chemical etching processes; the channel width (W) and length (L) were defined as 3000 μm and 20 μm, respectively.

The Poly(3-hexylthiophene) (P3HT) precursor was dissolved in tetralin solvent. This solvent was chosen over chloroform due to its slower evaporation rate, making it more suitable for our home-made jetting system. After jetting the OSC on circle type Au electrodes in air atmosphere, the device samples were annealed at 150 °C for 30 min in air, N_2 and solvent atmosphere.

The performances of OTFTs were measured by semiconductor parameter analyzer (HP4156C) in dark spaced probe station at room temperature.

3. Results and discussion

The field-effect mobility at $V_D=V_G$ was calculated by

$$I_{D,sat} = \left(\frac{W}{2L} \right) \mu C_i (V_G - V_T)^2 \quad (1)$$

where μ_{fe} is the field-effect carrier mobility, V_T is the threshold voltage, W is the channel width, L is the channel length, C_i is the capacitance per unit area.

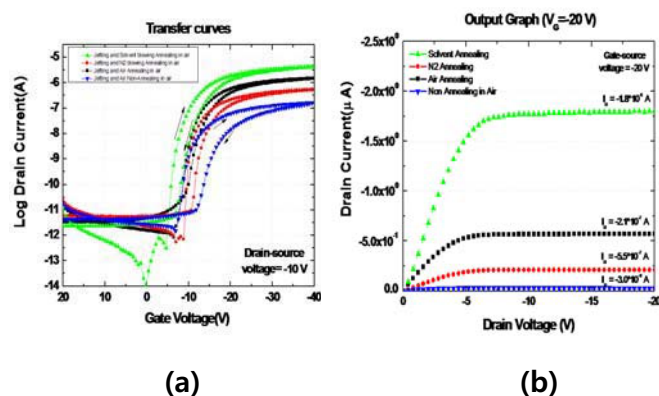


Figure 2. The electric characteristics of OTFTs with various processes (a) I_D - V_G , and (b) Output characteristics at $V_G=-20V$. ($W/L = 3000 \mu m/20 \mu m$)

Fig. 2 shows the electrical performances of the OTFT devices according to post annealing conditions. Without any self-assembled-monolayer (SAM) treatment and post annealing process, the field-effect mobility of OTFTs with jetting process in air atmosphere is much lower as $0.0002 \text{ cm}^2\text{V}^{-1}\text{s}^{-1}$; the lower field-effect mobility of the jetted OTFTs without annealing might correspond to poor film morphology looks like coffee stain near circle type source-drain electrode. On the other hand, the field-effect mobility of the jetted OTFTs can be improved by post annealing in air, N_2 and major solvent atmosphere; on current level is increased because the molecular of OSC are well rearranged onto SiO_2 during the post annealing process. Sub-threshold slope and on/off ratio are also improved. However, the result by N_2 annealing is inferior to that by air annealing process due to the effect of the directionality of N_2 blowing during. In our experiment, the solvent annealing drive best results as the field effect mobility (μ_{fe}) of $0.004 \text{ cm}^2\text{V}^{-1}\text{s}^{-1}$, the threshold voltage (V_T) of -7.9 V , the sub-threshold slope (S-S) of 0.98 V/dec and the on-off currents ratio (I_{on}/I_{off}) of 10^6 . In the case of output current, the solvent annealing can be improved more than 10 times compared to air annealing as shown in Fig. 2(b).

Table I. Summary of the electrical parameters for the OTFTs. μ_{fe} is the room temperature field-effect mobility, S is the sub-threshold swing, V_T is the threshold voltage.

Device	μ_{fe} ($\text{cm}^2\text{V}^{-1}\text{s}^{-1}$)	S (V/dec)	V_T (V)	I_{on}/I_{off}
(a) Non-Annealing in Air	0.0002	2.1	-8.6	10^4
(b) Air Annealing	0.002	1.0	-9.9	10^5
(c) N_2 Annealing	0.0009	1.1	-9.6	10^5
(d) Solvent Annealing	0.004	0.98	-7.9	10^6

4. Summary

For the jetting process, performances of the OTFT strongly depend on the molecular ordering of soluble OSC, which can be controlled by physical conditions of drying and post-annealing; in the case of solvent annealing, the well-defined molecular ordering of OSC can be achieved by optimizing physical conditions of annealing, but the useful solvent annealing process for the molecular ordering may not well developed, yet.

5. Acknowledgements

This work was supported by the Program for the Training of Graduate Students in Regional Innovation which was conducted by the Ministry of Commerce Industry and Energy of the Korean Government and a grant from the Information Display R&D center under the 21st Century Frontier R&D program.

6. References

- [1] C. D. Dimitrakopoulos, P. R. L. Malenfantols, *Adv. Mater.*, **14**, 99 (2004).
- [2] J. A. Lim, J. H. Cho, Y. D. Park, D. H. Kim, M. Hwang, K. Cho, *Appl. Phys. Lett.*, **88** (2006).
- [3] J. A. Lim, W. H. Lee, H. S. Lee, J. H. Lee, Y. D. Park and K. W. Cho, *Adv. Funct. Mater.*, **18**, 229-234 (2008).